International Journal of Applied Earth Observation and Geoinformation 136 (2025) 104310

Contents lists available at ScienceDirect

International Journal of Applied Earth Observation and Geoinformation

journal homepage: www.elsevier.com/locate/jag

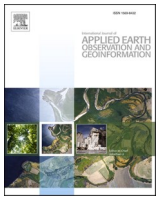

Scale effects in mangrove mapping from ultra-high-resolution remote sensing imagery

Hanwen Zhang [a,b], Shan Wei [a,b], Xindan Liang [a,b], Yiping Chen [c], Hongsheng Zhang [a,b,*]

[a] Department of Geography, The University of Hong Kong, Pokfulam, Hong Kong SAR, China
[b] The University of Hong Kong Shenzhen Institute of Research and Innovation, Shenzhen, China
[c] School of Geospatial Engineering and Science, Sun Yat-sen University, Zhuhai 519082, Guangdong, China

ARTICLE INFO

Keywords:
Mangrove forest
Fine-scale mapping
Deep learning
Scale effects
Hong Kong

ABSTRACT

Mangroves, critical for ecological sustainability, are challenging to map accurately due to their fragmented nature and difficult accessibility. Existing datasets, often constrained to 10 m or above resolutions, could misrepresent fragmented mangrove regions and suffer from sampling biases, limiting their regional applicability. Furthermore, scale conversion's spatial and statistical implications on mangrove mapping accuracy and area estimation remain largely unexplored. This study proposes a novel framework that leverages UHR (0.2 m) aerial photos and the DeepLabV3+ model for fine-scale mapping and systematically simulates and quantifies scale-induced effects. The resultant 20 cm-resolution mangrove map of Hong Kong achieved an overall accuracy (OA) of 92.1 %, with up to 53 % improvement compared to various existing datasets. It delineates complex boundaries in diverse coastal settings while preserving the structural integrity of fragmented patches. The total mangrove area in Hong Kong is estimated at ~720 ha, with Deep Bay comprising 77.5 %. The scale effects analysis revealed pronounced sensitivity in fragmented habitats, where each 1 m increase in resolution could result in an average area underestimation of 5000 m^2 and up to 25 % OA degradation when transitioning from 0.2 m to 30 m. Moreover, integrating patch geometry and scale responses indicated that 6 m is the optimal scale for monitoring. Beyond this, OA could sharply decline to below 82 % at the commonly used 10 m resolution and drop as low as 66 % at 30 m. These findings highlight the critical importance of fine-scale mapping using UHR images for effective mangrove conservation and management.

1. Introduction

Mangroves thrive in tropical and subtropical intertidal zones, playing vital roles in climate regulation, habitat stabilization, and shoreline protection. These ecosystems, composed of shrubs and small trees, support biodiversity and act as significant carbon sinks. They also offer natural protection against hurricanes, storms, and flooding, potentially preventing billions in damages (Bryan-Brown et al., 2020; Goldberg et al., 2020; Jia et al., 2023). Despite their ecological importance, mangroves are declining at a rate of 1–2 % annually, with a cumulative loss of 35 % over the past two decades due to sea-level rise, deforestation, land-use changes, and urban and agricultural expansion (Feller et al., 2017; Goldberg et al., 2020; Lovelock et al., 2015; Romañach et al., 2018). Therefore, accurate quantification of mangrove distribution is crucial for conservation, restoration, and risk assessment efforts.

Traditional field-based mapping methods are limited by accessibility, cost, and labor. Remote sensing has addressed these challenges, providing a crucial tool for large-scale mangrove mapping(Friess et al., 2019; Giri et al., 2011; Wang et al., 2019; Wei et al., 2024). Global datasets, including the 30 m Landsat-based MFW2000(Giri et al., 2011) and the Sentinel-2-based HGMF_2020 (Jia et al., 2023), have enhanced our understanding of mangrove distributions. However, these datasets often miss smaller or newly formed patches and are limited in their ability to differentiate between mangroves and other vegetation, due to coarse resolution (Wang et al., 2020; Zhang et al., 2021; Zhao and Qin, 2020).

In recent years, ultra-high-resolution (UHR) mapping, enabled by commercial satellites and UAVs, has significantly improved mangrove mapping at local and regional scales. Resolutions finer than 5 m from platforms such as WorldView-2, QuickBird, and IKONOS offer detailed mapping, especially for smaller mangrove patches(Guo et al., 2021; Mahdianpari et al., 2021). National-scale studies in China have shown

* Corresponding author at: Department of Geography, The University of Hong Kong, Pokfulam, Hong Kong SAR, China.
E-mail address: zhanghs@hku.hk (H. Zhang).

https://doi.org/10.1016/j.jag.2024.104310
Received 7 July 2024; Received in revised form 20 November 2024; Accepted 2 December 2024
Available online 20 December 2024

the advantages of sub-meter resolution for mangrove mapping, significantly improving accuracy and spatial detail compared to coarser global datasets (Tian et al., 2024; Zhang et al., 2021). While these fine-scale datasets address many limitations of global maps, they remain constrained by the cost, labor, and time required for data acquisition and ground truth validation, particularly in underrepresented coastal regions such as Hong Kong. Existing mangrove mapping efforts have largely relied on traditional machine learning techniques such as SVM and random forests, which depend on manual feature extraction from satellite or lidar data. While these methods have been widely used, they often struggle with spectrally similar classes, leading to accuracy drops in complex coastal environments(Jia et al., 2023; Mallick et al., 2021).

In recent years, deep learning-based mangrove mapping has achieved remarkable progress in wetland and coastal mangrove mapping. Y. Guo et al. (2021) utilized time-series Landsat data as input and integrated the classic Unet semantic segmentation with new network modules for large-scale mangrove mapping. Wang et al. (2023) proposed the Swin-UperNet model, which uses high-resolution optical images in Hainan to segment Spartina alterniflora and mangroves for invasive species studies. M. Guo et al. (2021) applied CNN for local reserve-scale mangrove mapping, using raw bands and extracted indices from Sentinel-2, outperforming traditional machine learning and pixel-based classification methods. A key advantage of deep learning methods is their ability to automatically learn features from data, eliminating manual extraction and simplifying training while effectively handling raw imagery(Zhao et al., 2024). However, these models are often restricted to multispectral data and face challenges such as slow training speeds and difficulties in fine boundary segmentation.

DeepLabV3+, a semantic segmentation algorithm introduced by Google in 2018, improves segmentation by adding a decoder structure to fuse shallow and deep features, refining the output. Compared to models such as Unet and SegNet, the main advantage of DeepLabV3+ lies in its use of atrous convolution, which expands the receptive field without losing information, enabling each convolution output to cover a larger area (Chen et al., 2017). This model has been successfully applied in classifying land cover types through detailed texture analysis, shape recognition, and edge reconstruction in complex imagery (Du et al., 2021; Gonzalez-Perez et al., 2022; He et al., 2024; Yao et al., 2019; Yu et al., 2022). However, its application in tropical and subtropical mangrove mapping remains limited. Recent studies have also shown the potential for handling large datasets using only RGB data while maintaining high classification accuracy. Fine-scale data from airborne sensors provide sufficient detail to differentiate mangroves from other coastal land cover types, overcoming the spectral similarity limitations of traditional methods(Carbonneau et al., 2020; Onishi and Ise, 2021). Nonetheless, applying the DeepLabV3+ model to segment mangroves from ultra-high-resolution RGB data remains largely unexplored.

The continued refinement of semantic segmentation techniques, alongside the integration of ultra-high-resolution (UHR) imagery, is poised to advance the study of scale effects in remote sensing. In this context, 'scale' refers to spatial resolution—the smallest distinguishable feature a sensor can detect (Aplin, n.d.; Feng et al., 2017; Marceau and Hay, 1999; Weng, n.d.; Woodcock and Strahler, 1987). According to Lam and Quattrochi (1992), scale operates on four levels: mapping, observation, measurement, and operation, each impacting remote sensing data application and analysis. Our study focuses on spatial resolution, crucial for accurate feature delineation in mangrove mapping. Scale effect, defined by the variability in features across different spatial resolutions, is a nuanced challenge in geoscience research. It gains significance as remote sensing data ranges from fine-scale to coarse resolution. Statistical methods show potential for addressing scale effects in vegetation mapping, yet remain underexplored. Our research introduces a novel approach to calculating and evaluating scale effects in mangrove mapping, employing fine-scale RGB imagery processed through deep learning-based segmentation to explore scale aggregation and transition implications.

The refinement of semantic segmentation techniques and the integration of ultra-high-resolution (UHR) imagery have the potential to advance the study of scale effects in remote sensing. In this context, *scale* refers to spatial resolution or the smallest distinguishable feature a sensor can detect (Aplin, n.d.; Feng et al., 2017; Lam and Quattrochi, 1992; Marceau and Hay, 1999). As Lam and Quattrochi (1992) noted, scale operates at four levels: mapping, observation, measurement, and operation, each influencing remote sensing applications. This study focuses on spatial resolution, critical for accurately delineating mangrove features, as scale effects—variations in feature detection across different resolutions—pose a significant challenge in geoscience. While statistical methods have been used to examine scale effects in vegetation mapping, few studies have explored these effects in the context of mangrove ecosystems(Lam and Quattrochi, 1992; Marceau and Hay, 1999). This study offers a novel approach to quantifying scale effects, employing fine-scale RGB imagery and deep learning-based segmentation to assess the spatial distribution and accuracy of mangrove mapping.

Despite the availability of existing mangrove datasets with varying map extents, their accuracy and performance at the regional level remain largely unvalidated, and the impact of scale on these products is still unclear. Hong Kong, as an important region with mangrove distribution, has long lacked comprehensive, high-resolution mangrove data. Our study aims to address this gap by leveraging 20 cm-resolution aerial imagery and advanced deep learning techniques to produce an updated and detailed mangrove map (UHRHKM) and investigate how scale influences classification results. Specifically, we aim to (1) evaluate the performance of DeepLabV3+ through accuracy assessments; (2) analyze the effects of scale based on fine-scale segmentation results; and (3) compare the UHRHKM map with the existing mangrove dataset. By addressing the need for high-resolution data and the challenges of scale, our study aims to deepen the understanding of mangrove spatial distribution and examines the impact of scales on segmentation accuracy. Through these efforts, we seek to facilitate the creation of more effective conservation and management strategies, while enabling further applications biophysical characteristics mapping applications.

2. Study area and data preparation

2.1. Study area

The study area focuses on the coastal regions of Hong Kong, located in southeastern China at the mouth of the Pearl River Delta, near major cities such as Shenzhen and Guangzhou (Fig. 1). Hong Kong, a key component of the Greater Bay Area, is characterized by around 60 mangrove stands across six districts: Sai Kung, Northeast New Territories, Tolo Harbour, Deep Bay, Lantau Island, and Hong Kong Island. The region's varied topography, including mountainous areas and flat coastal plains, influences the distribution and health of mangrove ecosystems. These coastal environments are affected by the Pearl River and South China Sea, impacting salinity levels and sediment deposition. Hong Kong's subtropical climate, with hot, humid summers and mild, dry winters, supports mangrove growth. These forests are crucial coastal wetlands, providing habitats, biodiversity conservation, carbon sequestration, and coastal defense. Despite their importance, mangroves in Hong Kong face threats from urban development and pollution.

2.2. Data preparation

2.2.1. Reprocessing of ultra-high-resolution (UHR) images

In this study, we utilized a subset of the DOP5000 series, an orthorectified aerial photography dataset produced by the Lands Department of Hong Kong. DOP5000 provides a high-resolution ground sample distance of 0.2 m per pixel, derived from aerial photographs taken at altitudes of 2,000 to 9,000 feet. The dataset is geographically referenced to the Hong Kong 1980 Grid system and provided in GeoTIFF format, with each tile consisting of 18,750 by 15,000 pixels and a file

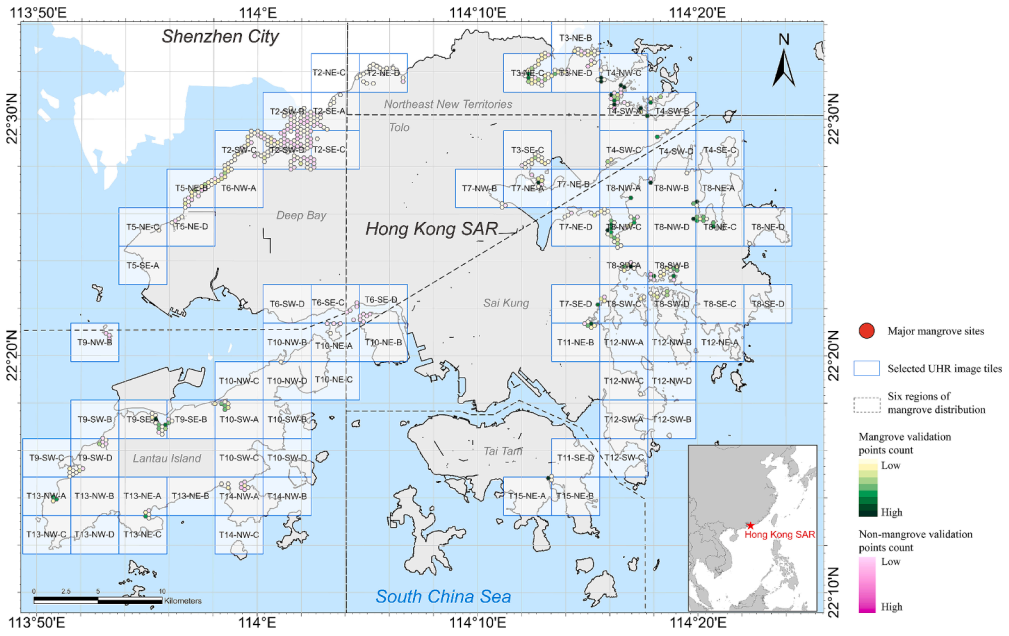

Fig. 1. Location and distribution of validation points of the study.

size of approximately 810 MB. Employing digital photogrammetry and geometric correction techniques, DOP5000 ensures images are free from distortions due to camera tilt and topographic relief. For our study, we acquired 81 tiles covering Hong Kong's coastal areas, capturing regions with potential mangrove and mudflat distributions. These images, captured in three RGB bands, offer detailed visual data conducive to thorough vegetation analysis and fine-scale mangrove mapping. The selected images and study area are shown in Fig. 1, with 90.1 % of the images taken between 2019 and 2023. Detailed acquisition dates and year distribution are provided in Table 1.

2.2.2. Sample dataset preparation

Labels were annotated from two sources: ground truth surveys in accessible mangrove areas and UHR image interpretation for inaccessible regions, both verified by experts. This labeling process was essential for training accurate semantic segmentation models.

Samples were collected from across Hong Kong, representing diverse habitat characteristics such as species composition and different mangrove patch types. Special attention was given to ecologically significant and protected areas, including the Mai Po Ramsar Site in Deep Bay, as well as three Sites of Special Scientific Interest (SSSI): Lai Chi Wo within the Yankee Chau Tong Marine Park, Ting Kok in Tolo Harbour, and Hoi Ha Wan mangroves in Hoi Ha Wan Marine Park. These areas were prioritized to capture representative features of Hong Kong's mangroves (Fig. 1). In this study, the sampling was designed to cover the majority of the 60+ officially recorded mangrove sites by the government (https://www.afcd.gov.hk/), ensuring a balanced and spatially even distribution across the entire study area.

To account for the complexity and variability of the dataset, data augmentation techniques such as cropping, rotating, scaling, and normalization were applied (Gonzalez-Perez et al., 2022; Guo et al., 2021). Training tiles were generated by extracting 256 × 256 pixel image-label pairs with a 128-pixel stride and 90°, 180°, and 270° rotation angles. The dataset was then split into training, validation, and test sets in a ratio of 8:1:1, resulting in a total of 3959 images for comprehensive model evaluation.

Table 1
Acquired dates of the applied UHR aerial photo dataset.

Acquisition year	Number of tiles	Percentage
2017	8	9.9 %
2019	8	9.9 %
2021	2	2.5 %
2020	26	32.1 %
2023	37	45.7 %
Sum	81	100 %

3. Methodology

3.1. Deep learning semantic segmentation models

3.1.1. DeepLabv3+ model and training

The DeepLabv3+ model, introduced in 2018, is widely recognized for its effectiveness in semantic segmentation tasks, particularly in land-use classification, due to its encoder-decoder structure and enhanced multi-scale contextual feature fusion (Chen et al., 2018; Du et al., 2021). In this study, we adopted DeepLabv3+ with a key enhancement: replacing the original Xception backbone with MobileNetV2 for improved computational efficiency and faster training (Howard et al., 2018; Gonzalez-Perez et al., 2022). MobileNetV2, designed for lightweight applications, utilizes depthwise separable convolutions, inverted residuals, and a linear bottleneck structure to reduce the model's parameter count while maintaining high accuracy, making it suitable for large-scale mapping tasks. For training, the backbone parameters were frozen after accuracy plateaued to optimize resource use. The model was trained for 200 epochs with a batch size of 16 and an initial learning rate of 0.001, managed dynamically across epochs. The Adam optimizer was employed to balance computational efficiency and performance (Guo et al., 2021). As the model takes 256 × 256 pixel images, the structure and parameter settings of the used backbone model are presented in Fig. 2 and Table 2.

Then we applied a frozen-stage strategy, where the backbone remains fixed once accuracy plateaus to optimize resource use. The model was trained for 200 epochs with a batch size of 16. An initial learning rate of 0.001 was set, and controlled automatically by training epochs (Hong et al., 2024; Vieilledent et al., 2018; Yao et al., 2019). The Adam optimizer was chosen for its computational efficiency and low memory requirements (Guo et al., 2021; Wang et al., 2023).

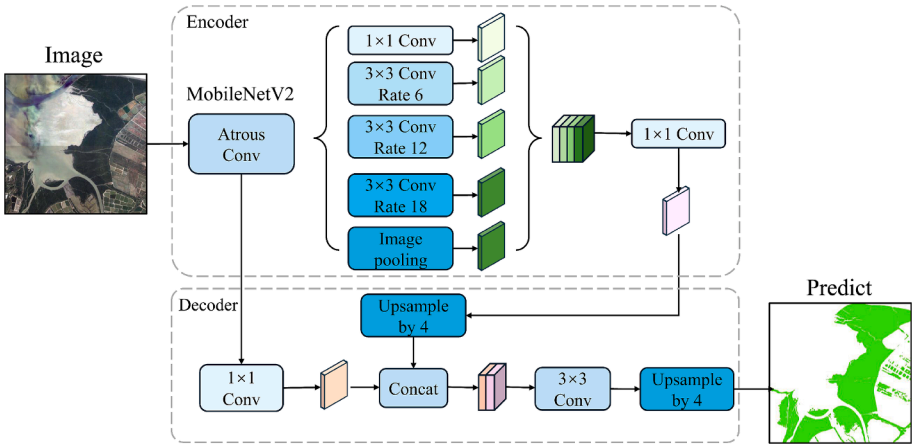

Fig. 2. Diagram of the applied DeepLabV3+ network.

Table 2
MobileNetV2 network structure.

Input	Operator	t	c	n	s
256××256 × 3	Conv2d	–	32	1	2
128 × 128 × 32	Bottleneck	1	16	1	1
128 × 128 × 16	Bottleneck	6	24	2	2
64 × 64 × 24	Bottleneck	6	32	3	2
32 × 32 × 32	Bottleneck	6	64	4	2
16 × 16 × 64	Bottleneck	6	96	3	1
16 × 16 × 96	Bottleneck	6	160	3	2
8 × 8 × 160	Bottleneck	6	320	1	1
8 × 8 × 320	Conv2d 1 × 1	–	1280	1	1
8 × 8 × 1280	Avgpool 8 × 8	–	–	1	–
1 × 1 × k	Conv2d 1 × 1	–	k	–	–

3.1.2. Comparison models

To evaluate segmentation performance, this study selected U-Net and PSPNet as benchmark models alongside the proposed DeepLabV3+ model.

U-Net is a widely used convolutional neural network designed for semantic segmentation tasks, particularly effective in biomedical and environmental applications. Its encoder-decoder structure facilitates the extraction of multiscale features, while skip connections ensure that spatial information from earlier layers is preserved during upsampling. U-Net is known for its simplicity and adaptability, making it a standard benchmark for segmentation tasks in various domains. For this study, the structural details of U-Net are omitted for brevity.

PSPNet (Pyramid Scene Parsing Network) is another prominent model designed to enhance feature extraction through its pyramid pooling module, which captures contextual information at multiple scales. This architecture allows PSPNet to excel in identifying large-scale objects and distinguishing between closely related classes. Despite its strength in handling multiscale features, PSPNet often struggles with fine-grained segmentation tasks, particularly in scenarios involving fragmented or narrow structures. The technical details of Unet and PSPNet's architecture are not elaborated in this study to maintain a focus on comparative analysis.

3.2. Post-classification processing and validation

3.2.1. Post-classification processing

After generating the initial mangrove classification maps using the DeepLabv3+ model, we adopted several post-processing steps o refine the results and improve classification consistency. Morphological operations were applied to consolidate mangrove patches by filling small gaps and removing isolated noise elements. For areas where class confusion between mangroves and other vegetation occurred, we employed a context-driven relabeling process based on the spatial patterns characteristic of mangrove ecosystems.

3.2.2. Performance evaluation

This study also includes a comparison of accuracy with existing mangrove maps. Since the focus is on mangrove mapping precision, all non-mangrove classes were merged into a single category for the validation points. Specifically, we randomly generated 1,500 validation points each for mangroves and non-mangroves, both within the model results and within a 10 m buffer zone near the edges of mangrove patches, considering the common resolution of fine-scale mangrove maps. These points were evenly distributed across different types of coastal areas with varying regional characteristics. The distribution of the validation samples is shown in Fig. 1. We then evaluate the performance of our mangrove segmentation and recognition model using several key metrics: Overall Accuracy (OA), Precision, Recall, F1 Score, and Cohen's Kappa.

3.3. Scale effect analysis

The scale effects analysis in this study comprises three components: input data, the scaling calculation process, and the evaluation of scaled mangrove distribution layers. The input data originate from the ultra-high-resolution (20 cm per pixel) mangrove segmentation raster produced by the deep learning model described in Section 3.2. We then generate a series of scale-transformed mangrove distribution layers through spatial aggregation analysis of neighborhoods using various scale factors. The spatial aggregation process follows the formula:

$$\mathrm{R(i,\ j)} = \frac{1}{\mathrm{N}} \sum_{\mathrm{n=1}}^{\mathrm{N}} I(n) \tag{8}$$

where $R(i,j)$ represents the resampled value at the new scale for the pixel at (i,j), N is the total number of original high-resolution pixels within the new coarse pixel, and $I(n)$ is the binary indicator for mangrove presence in the n^{th} high-resolution pixel. The scale factor S adjusts the neighborhood size for aggregation:

$$S = \frac{\textit{desired scale resolution}}{\textit{original scale resolution}} \tag{9}$$

The variable S is used to adjust the size of the neighborhood for aggregation, thereby transforming the original high-resolution data to the desired coarser scale. For each round of transformation, a series of threshold T is applied to the area percentage of mangrove presence:

$$M(i,j) = \begin{cases} 1 & \text{if } R(i,j) \geqslant T,\ T \in \{0.1, 0.2, ..., 1.0\} \\ 0 & \text{if } R(i,j) < T \end{cases} \tag{10}$$

where $M(i,j)$ represents the final classification of mangrove presence

in a coarse pixel, determined by the most dominant class within that pixel. T reflects the proportion of mangrove coverage within a scale-transformed cell, with values ranging from 0 to 1. Higher T values indicate a greater likelihood of the cell being classified as mangrove, with $T = 1$ requiring full coverage to classify as mangrove, and $T = 0$ requiring full coverage to classify as non-mangrove. To balance computational efficiency with the objectives of this analysis, we applied threshold intervals of 0.1 (i.e., 10 %, 20 %, … 100 %). The average value was used to represent overall mangrove distribution and explore the impact of different thresholds on classification accuracy (Camacho Olmedo et al., 2017; Feng et al., 2017; Weng, n.d.).

The scaling process was standardized from 20 cm to 1 m, then increased in 1 m intervals up to 30 m, the typical upper limit in mangrove remote sensing. To assess scale effects, we quantified the impact on mangrove classification using four metrics: area, OA, UA, and PA, based on previously described validation points. The optimal observational scale was identified at the inflection point where a noticeable slope change indicated the most effective resolution for mangrove analysis.

4. Results

4.1. Accuracy assessment of the mangrove map of Hong Kong in 2024

The confusion matrix and accuracy assessment of the ultra-high-resolution Hong Kong mangrove map (UHRHKM) for 2024 demonstrate excellent performance (Fig. 3). All evaluation metrics, including overall accuracy (OA), precision, recall, F1 score, and Kappa coefficient, exceed 0.90. The OA for the entire Hong Kong map reaches 0.921, with regional validation showing that most areas achieve OA values above 0.90, except for Lantau Island with a slightly lower OA of 0.869. Additionally, the model proves highly reliable in areas with limited samples. For example, in Tai Tam, where only a single mangrove habitat exists, the OA remains high at 0.919 (Fig. 3). The Kappa coefficient of 0.941 indicates strong agreement between mapped pixels and ground-truth data, affirming the high accuracy of UHRHKM. These results demonstrate robustness and consistency across varied conditions in Hong Kong.

4.2. Areas and spatial distribution of Hong Kong mangroves in 2024

The study mapped mangrove distribution across Hong Kong in 2024, revealing a total mangrove area of 720.2 ha(Fig. 4). Deep Bay hosts the largest share, accounting for 77.5 % of the total mangrove area, followed by Sai Kung, the Northeast New Territories, Lantau Island, and Tolo. On Hong Kong Island, Tai Tam is the only mangrove habitat, covering just 0.2 % of the total area (Fig. 4(a)). We then calculated patch numbers and median patch areas for the six regions. Median patch areas were used instead of mean values to minimize the influence of extremely large patches, predominantly found in Mai Po, ensuring an objective reflection of patch characteristics (Fig. 4(b)). Patch counts were sorted in descending order to highlight differences in patch abundance and area across regions. Additionally, Fig. 4(c) illustrates the spatial distribution of patches categorized by area classes. The results reveal that Sai Kung exhibits the largest median patch size (449.8 m^2), with patch counts comparable to those in Deep Bay(329 compared to 328 patches). Interestingly, the three eastern regions—Northeast New Territories, Tolo, and Sai Kung—where mangroves thrive on sandier coasts and ports with less sediment deposition, have larger average patch areas compared to Deep Bay (381.2 m^2 compared to 346.3 m^2). This finding is particularly noteworthy as Deep Bay is traditionally regarded as the most mangrove-rich region in Hong Kong. In contrast, mangroves along the east coast have received less attention and are often underappreciated.

Mangroves in Hong Kong are mainly found in estuaries and bays (Fig. 5). We selected one representative region of interest from each of

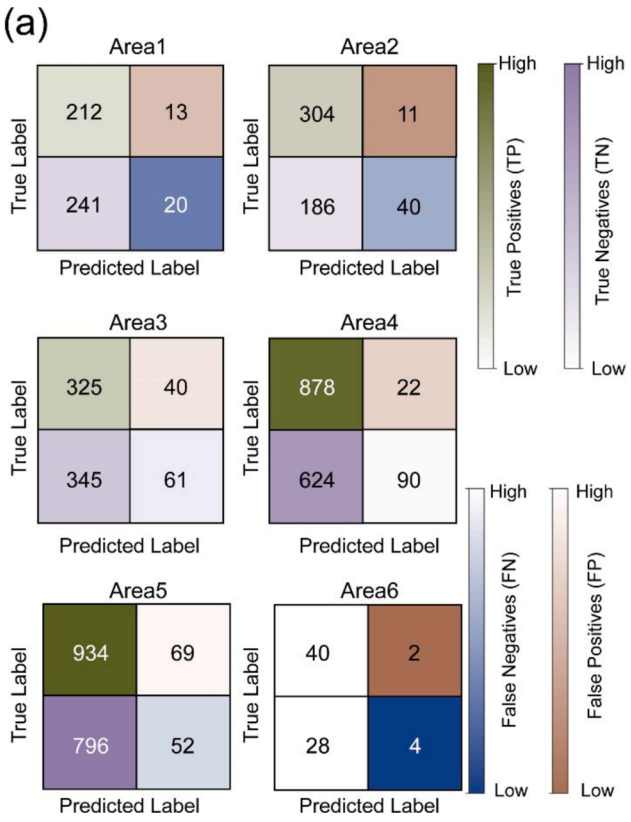

(b)

Accuracy	
Overall	0.921
Precision	0.945
Recall	0.910
F1 score	0.927
Kappa	0.941

Accuracy By Regions (OA)	
1	0.932
2	0.906
3	0.869
4	0.931
5	0.934
6	0.919

Fig. 3. Accuracy assessment across six regions: (a) Confusion matrix by region (1 – Tolo, 2 – Deep Bay, 3 – Lantau Island, 4 – Northeast New Territories, 5 – Sai Kung, 6 – Tai Tam); (b) Summary of OA, precision, recall, F1 score, kappa, and regional accuracies.

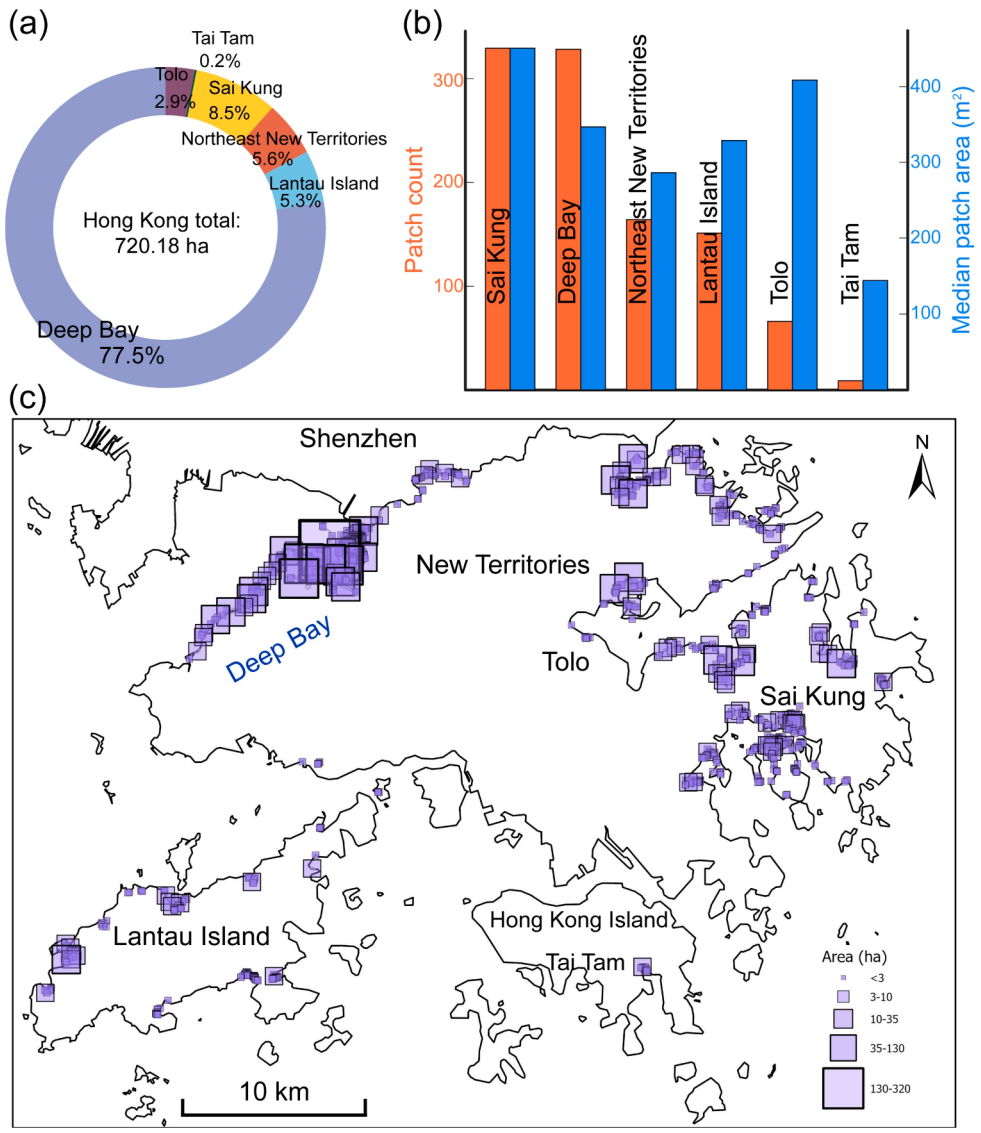

Fig. 4. Area and patch characteristics of Hong Kong's mangroves in 2024.(a) Proportional area distribution of mangroves by region, (b) patch count and median patch area for the six regions, and (c) spatial distribution of patches with symbols indicating different habitat area ranges.

the six mangrove regions in Hong Kong. Each of the selected sites showcases unique habitat characteristics or holds special conservation value to offer a clear view of mangrove distribution across varied environments. Ting Kok, near Tolo Harbour, is one of the largest mangrove areas in Hong Kong. It has been designated a Site of Special Scientific Interest (SSSI) since 1985 due to its ecological importance, coarse sandy substrate, and high salinity environment (Fig. 5(a)). Mai Po, a Ramsar-listed wetland, is a globally significant mangrove habitat (Fig. 5(b)). Tai O's mangroves, surrounding traditional stilt houses, highlight the interaction between mangroves and human activities (Fig. 5(c)). The mangroves in Lai Chi Wo are near Yan Chau Tong Marine Park (Fig. 5 (d)). Sai Keng, located in the Kat O Hoi area, benefits from significant freshwater inflow (Fig. 5(e)). Tai Tam, on Hong Kong Island, is the last remaining mangrove stand in this region and grows on rocky marshes and sandy beaches. It is also designated as an SSSI. The segmentation results confirm that the 0.2 m-resolution map effectively identifies mangrove patches across different habitats. The map maintains clear and accurate boundaries in complex areas such as mudflats, sandy beaches, marshes, and built-up zones (Fig. 5). It also captures fine details within large patches, including internal creek networks and fragmented habitats. These results highlight the map's precision and ability to represent mangrove spatial characteristics with high accuracy.

4.3. Scale effects based on fine-scale segmentation

4.3.1. Accuracy trends and area estimation

Accuracy metrics (OA, UA, PA) across six regions, shown in Fig. 6, highlight the distinct scale-dependent responses of mangrove habitats. Fragmented regions such as Tolo and Northeast New Territories exhibit pronounced accuracy declines as resolution coarsens. OA of 91.9–93.4 % at fine scales in these areas drops sharply to 68.8–72.1 % at 30 m, indicating significant challenges in classifying fragmented mangrove patches at coarser scales. Area estimation trends, presented in Fig. 7, further emphasize the scale sensitivity of fragmented regions. Sai Kung experiences substantial area underestimation, with a loss of 27–38 % at 30 m. By comparison, Deep Bay shows a much smaller reduction of 3.47 %. Regression analysis confirms that fragmented regions experience faster area loss rates (e.g., Sai Kung: $y = -0.88x + 66.68$) compared to continuous areas (e.g., Deep Bay: $y = -0.73x + 556.65$).

4.3.2. Patch geometric characteristics and optimal observation scale

Patch width, as a key geometric characteristic of mangroves

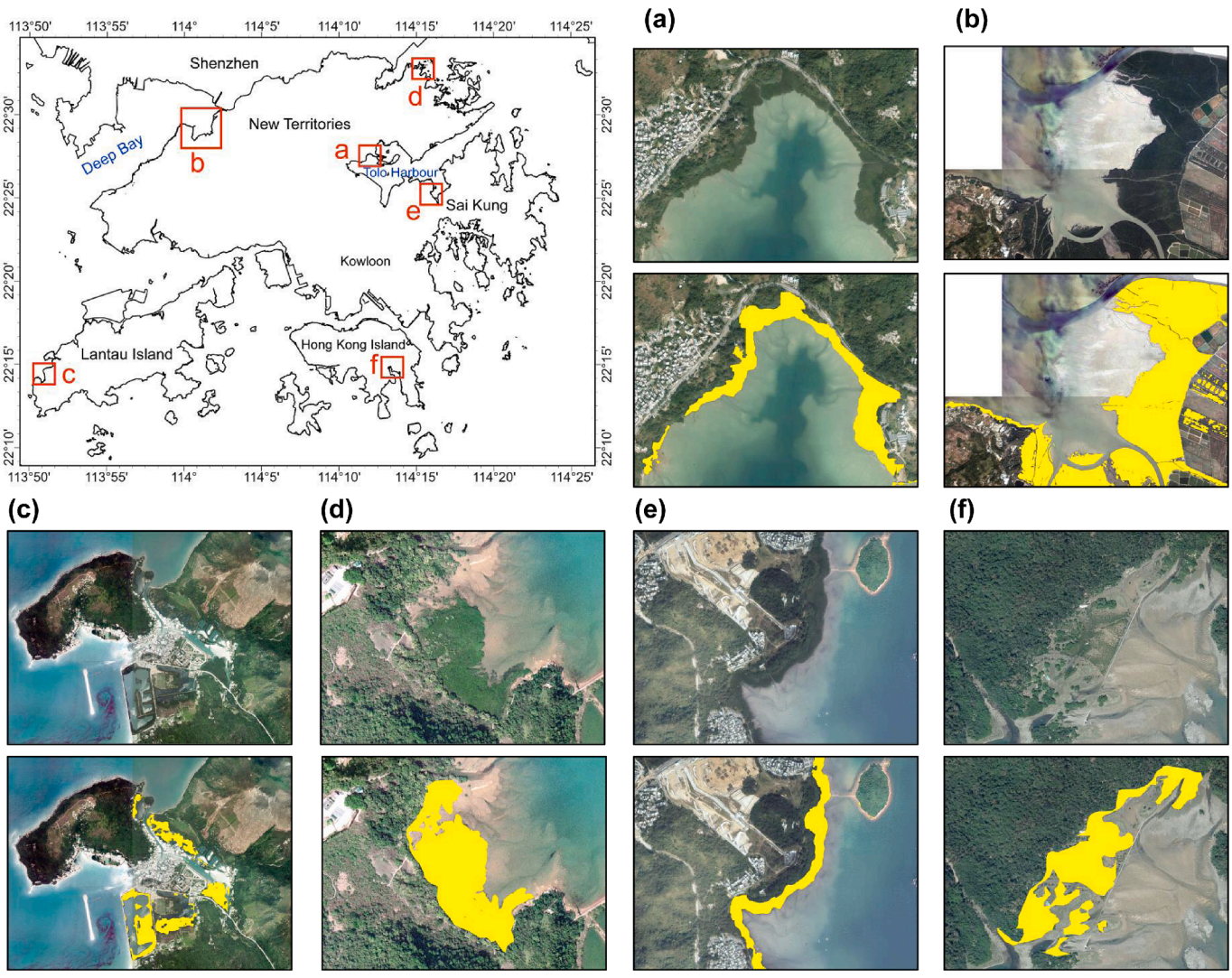

Fig. 5. Regional examples of aerial photos and segmentation results across Hong Kong. (a) Ting Kok in Tolo, (b) Mai Po and adjacent mangrove stands in Deep Bay, (c) Tai O in Lantau Island, (d) Lai Chi Wo in Northeast New Territories, (e) Sai Keng in Sai Kung, and (f) Tai Tam in Hong Kong Island.

distributed stretching the coastlines, could explain the scale sensitivity observed in mangrove mapping across regions. To minimize the influence of extremely large patches, the median patch width was used as the representative metric. In fragmented regions like Tai Tam (3.8 m) and Northeast New Territories (5.1 m), the median patch widths are comparable to or smaller than pixel sizes at coarser resolutions, likely resulting in patch merging and misclassification. In contrast, regions with wider patches, such as Sai Kung (6.5 m) and Deep Bay (5.6 m), retain higher segmentation accuracy at 6 m resolution. However, over-generalization becomes apparent at resolutions of 10 m and beyond, leading to a loss of spatial detail and classification reliability. These geometric insights align with accuracy trends in Fig. 6, where 6 m emerges as a critical threshold across all regions. Below this scale, segmentation retains sufficient detail to capture fragmented and linear features. However, beyond 6 m, accuracy deteriorates rapidly and drops by 10–15 % from descending to 10 m-scale.

4.3.3. *Habitat-specific scale responses*

To further illustrate these scale effects, we analyzed three representative sites: fragmented patches in Chek Keng, pond-based mangroves in Ha Pak Nai, and linear mangroves in Tsim Bei Tsui (Fig. 8(a)-(c)). Accuracy and area changes for these sites are summarized in Table 3. These sites highlight the spatial and accuracy effects of scale conversion at 6 m, 10 m, and 30 m. At 6 m resolution, mapping maintains acceptable accuracy, with OA ranging from 92.4 % to 95.2 %, reflecting moderate losses in edge sharpness. However, at 10 m resolution, OA declines to 82.4 %-86.1 %, and area errors become noticeable. For example, Chek Keng shows an area decrease of 2994.5 m^2, while Ha Pak Nai experiences a decrease of 133.6 m^2. At 30 m resolution, over-generalization leads to further spatial distortions. Chek Keng exhibits a substantial OA reduction of 66.4 %, while Tsim Bei Tsui's area is overestimated by 5652.3 m2 due to linear features being misrepresented as blocky structures.

4.4. *Comparisons with existing mangrove datasets*

The comparative analysis (Table 4, Fig. 9) highlights variations in mapping performance across global, national, and regional datasets when applied to selected ecologically complex regions. Omission errors are prevalent in global datasets such as GMW_V3 (30 m resolution), which struggle to delineate mangrove boundaries in tidal flats and creek systems, exemplified by the challenges in accurately mapping the Mai Po Wetland (Fig. 10(a)). These limitations are likely due to mixed pixel effects and insufficient spatial resolution. National datasets, such as MC2018 (2 m resolution), show improved performance but still fail to capture fragmented habitats effectively, especially in remote areas such

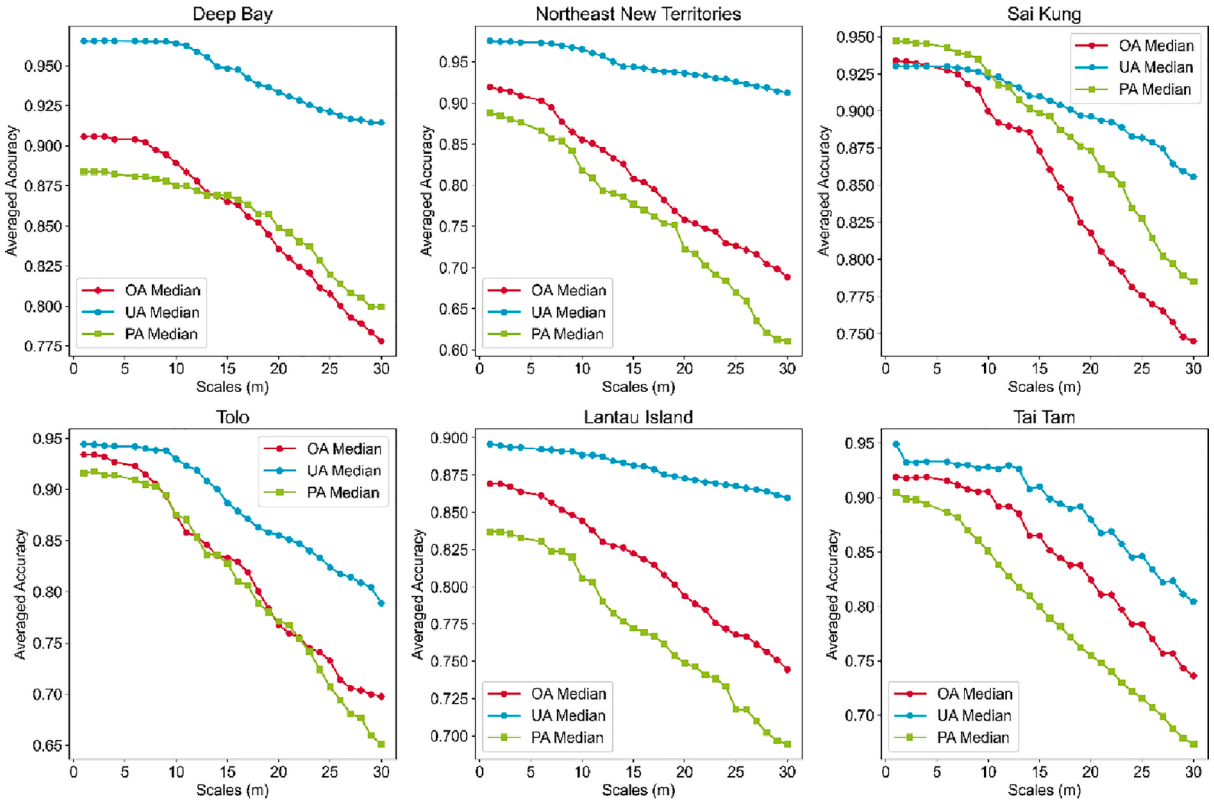

Fig. 6. Accuracy metrics by scale for mangrove classification in Hong Kong.

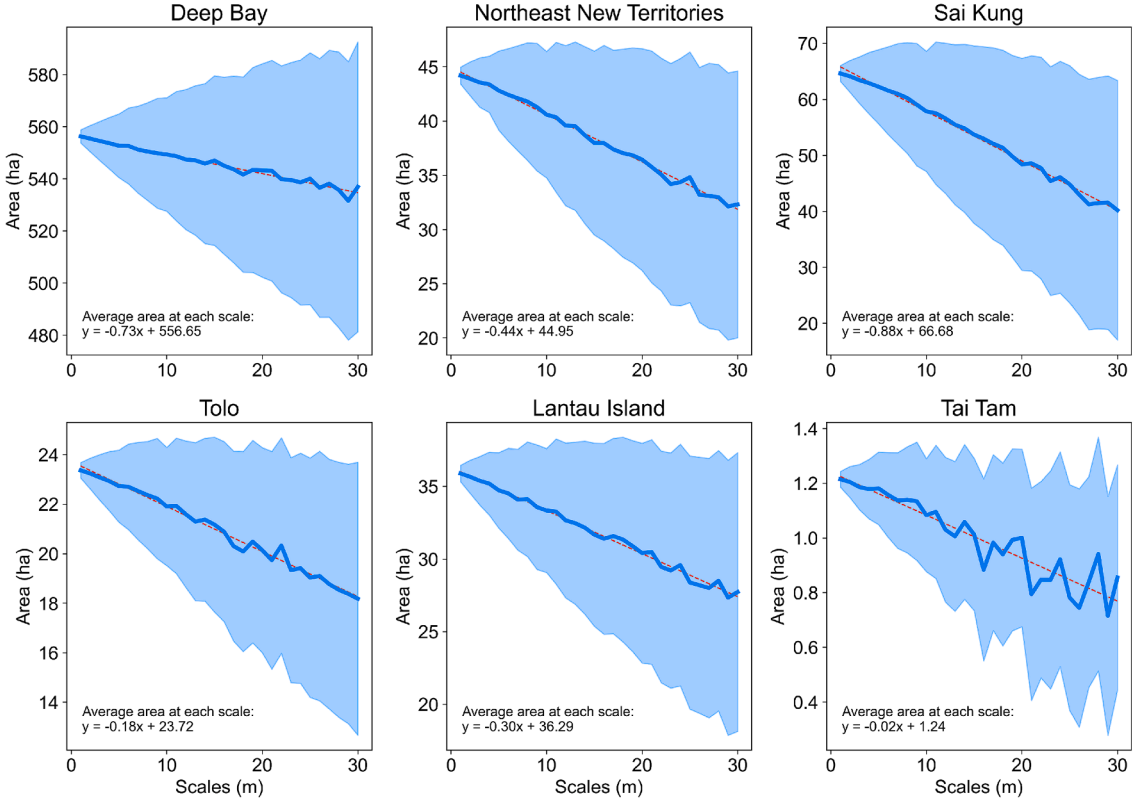

Fig. 7. Scale-dependent variations in mangrove area across six regions of the study area. The blue lines indicate the average mangrove area at each scale, with the blue-shaded regions representing the standard deviation STD range. The red dashed lines represent the fitted linear regression equations for the average area changes. (For interpretation of the references to colour in this figure legend, the reader is referred to the web version of this article.)

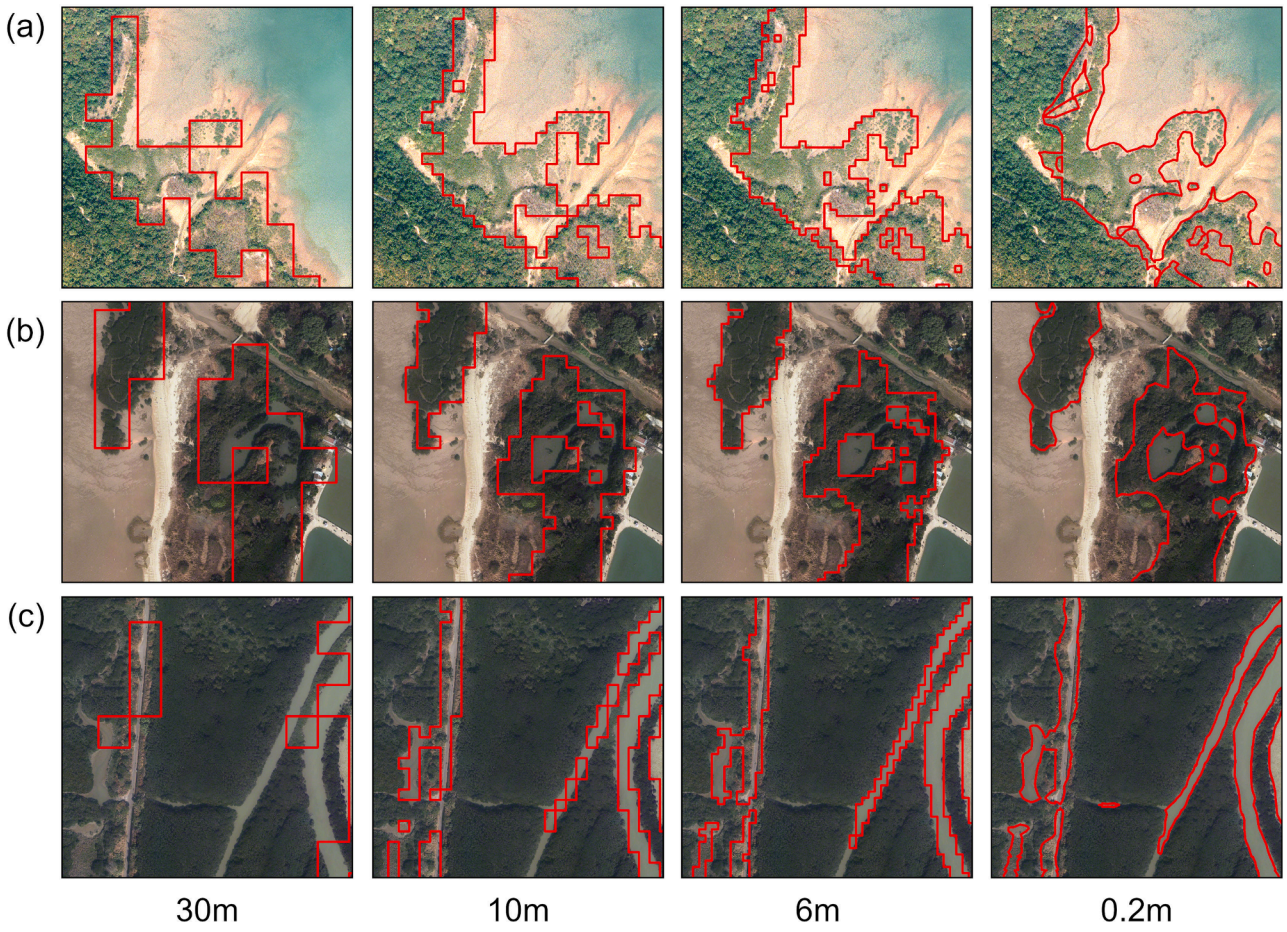

Fig. 8. Spatial demonstrations of effects of scale conversion mangrove mapping at typical sites: (a) Chek Keng, (b) Ha Pak Nai, and (c) Tsim Bei Tsui. The red line indicates mangrove extraction boundaries. (For interpretation of the references to colour in this figure legend, the reader is referred to the web version of this article.)

Table 3
Accuracy and area response to scale changes in mangrove mapping at selected sites.

	Chek Keng		Ha Pak Nai		Tsim Bei Tsui	
	OA (%)	Area change (m^2)	OA (%)	Area change (m^2)	OA (%)	Area change (m^2)
0.2 m	98.4	0.0	96.7	0.0	98.8	0.0
6 m	92.4	−2098.5	93.3	−1.6	95.2	−359.7
10 m	83.6	−2994.5	82.4	−133.6	86.1	−847.7
30 m	66.4	2905.5	66.2	−433.6	67.3	5652.3

Table 4
Overview of mangrove datasets used in comparative analysis.

Map product	Year	Authors	Map extent	Scale (m)
GMW_V3	2022	Bunting et al.	Global	30
WorldCover_V2	2021	European Space Agency	Global	10
HGMF	2020	Jia et al.	Global	10
LREIS_GLOBALMANGROVE	2020	Xiao et al.	Global	10
Zhao&Qin	2020	Zhao et al.	National	10
MC2018	2018	Zhang et al.	National	2
LSMM	2024	Tian et al.	National	0.9
LUMHK_RasterGrid_2022	2022	Planning Department of Hong Kong	Regional	10
UHRHKM (This study)	2024	Zhang et al.	Regional	0.2

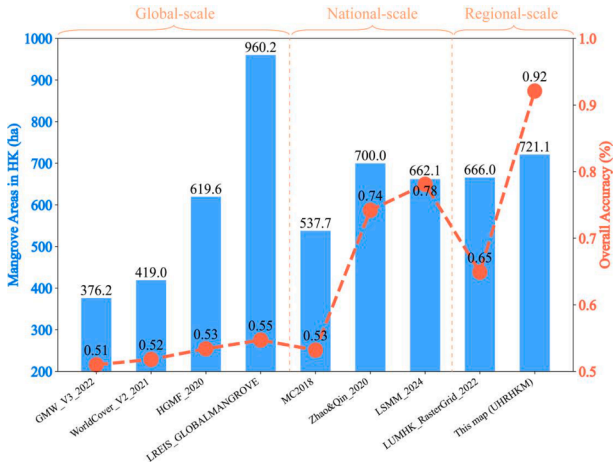

Fig. 9. Comparative analysis of accuracy and area in mangrove mapping datasets.

as Sam Nga Hau (Fig. 10(d)). Misclassification errors remain an issue even in finer-resolution datasets. For example, while LSMM (0.9 m resolution) improves patch continuity, it occasionally fragments connected patches in areas with complex terrain. This indicates persistent difficulties in representing heterogeneous mangrove landscapes. The UHRHKM map (0.2 m resolution) produced in this study addresses these challenges. It captures fragmented habitats and intricate tidal creeks with greater detail, maintaining edge sharpness and patch completeness,

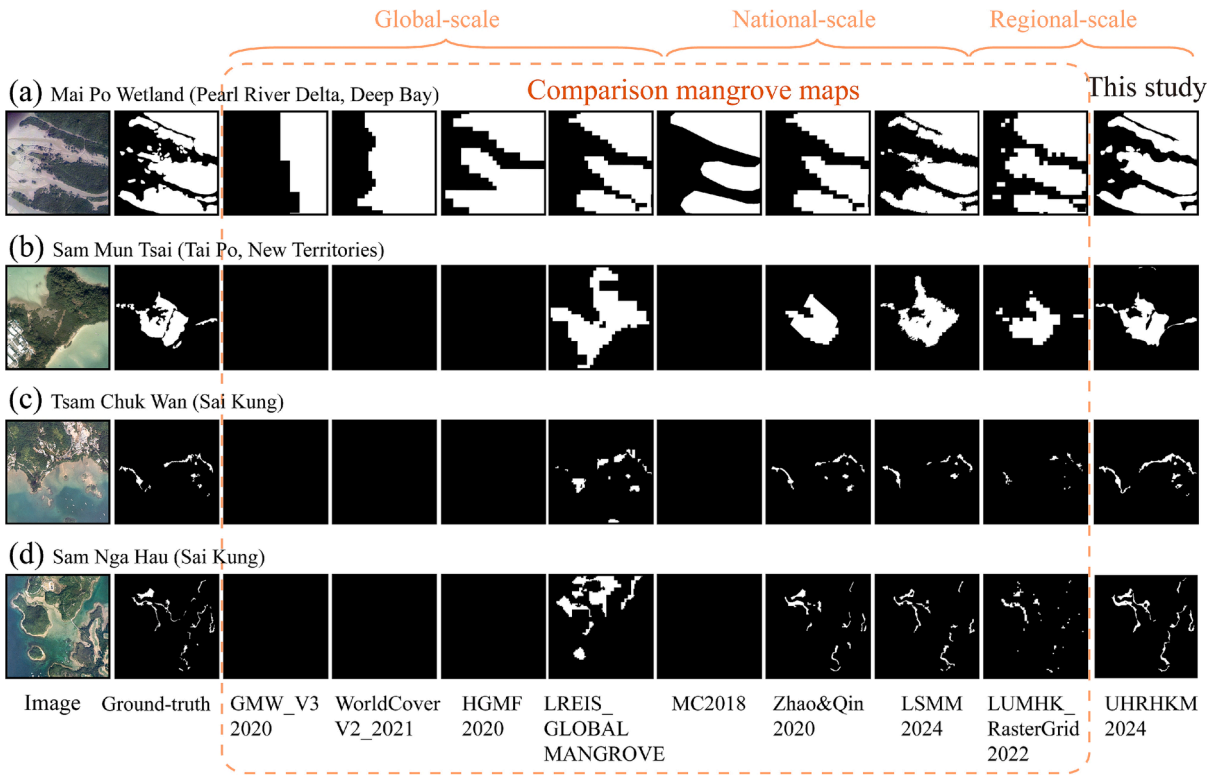

Fig. 10. Comparison of mangrove distribution maps from various sources in typical regions.

particularly along the east coast. These advantages provide a more reliable spatial representation and improve the accuracy of area estimates in ecologically diverse mangrove regions.

5. Discussion

5.1. Scale-induced errors in mangrove mapping and its possible reasons

This study proposes a systematic quantification framework to examine the effects of scale changes on mangrove mapping accuracy and spatial area. By systematically aggregating ultra-high-resolution (0.2 m) binary classification results to coarser resolutions (e.g., 1 m, 6 m, 10 m, 30 m) using a majority aggregation method, the framework simulates lower-resolution distributions and evaluates how scale influences mapping outcomes. Majority aggregation ensures the preservation of the dominant land-cover class within each resampling window, minimizing distortions caused by mixed pixels and ensuring consistency in binary classifications. By approximating real-world mapping challenges, this approach highlights the critical issues of spatial detail loss, precision degradation, and area estimation errors at coarser scales. Through this approach, we demonstrated the high sensitivity of mangrove mapping to scale changes, with significant accuracy loss and area misestimation observed at lower resolutions, particularly in fragmented habitats (Figs. 6–8, Table 3).

Through integrating ecological perspectives, such as patch geometry, the framework identifies key thresholds where spatial detail and classification reliability begin to degrade. For instance, in fragmented habitats where mangrove patch widths approach or fall below pixel sizes, boundary-blurring and patch merging become prominent due to mixed pixel effects (Fig. 8). These findings underscore the importance of high-resolution monitoring to retain critical spatial detail and classification accuracy. The observed trends (e.g., accuracy degradation by 10–15 % from 1 m to 10 m resolution, as shown in Fig. 6) emphasize the need for a balanced approach in selecting observation scales, particularly for ecologically fragmented regions. At selected sites, spatial comparisons (Table 3) demonstrate how scale effects influence area and accuracy, highlighting the variability in mangrove patch characteristics across regions.

While this framework proposes new insights into scale-induced effects, further refinements could address the remaining challenges. Incorporating advanced aggregation algorithms, such as weighted methods based on patch morphology, and integrating additional data types, such as spectral or structural features, would improve the precision of scale-effect analyses. These advancements could provide a more comprehensive understanding of how scale affects mangrove distributions and lead to improved models that better support ecological conservation and management efforts.

5.2. Model performance, challenges, and future work

This study is the first attempt to apply deep learning methods for mangrove segmentation in Hong Kong, achieving great improvements over existing datasets. The DeepLabV3+ model demonstrated strong performance, with overall accuracy (OA), precision, and F1 scores reaching 92.1 %, 94.5 %, and 92.7 %, respectively. Compared to other models like UNet, PSPNet, and DeeplabV2, it achieved significant improvements in precision, surpassing DeeplabV2 by 24.83 %, PSPNet by 16.4 %, and UNet by 9.1 %. However, slightly lower PA values highlight areas where further refinement is needed (Table 5).

Examples of segmentation results across various models in Fig. 11 highlight the spatial advantages of the DeepLabV3+ model. Four sites with distinct environmental settings were analyzed: a sediment-rich

Table 5
Accuracy comparison of different mangrove segmentation models.

Model	OA	Precision	Recall	F1 score
DeeplabV2	0.916	0.757	0.937	0.853
Unet	0.903	0.854	0.97	0.845
PSPnet	0.92	0.786	0.975	0.87
Improved DeeplabV3+	**0.921**	**0.945**	**0.91**	**0.927**

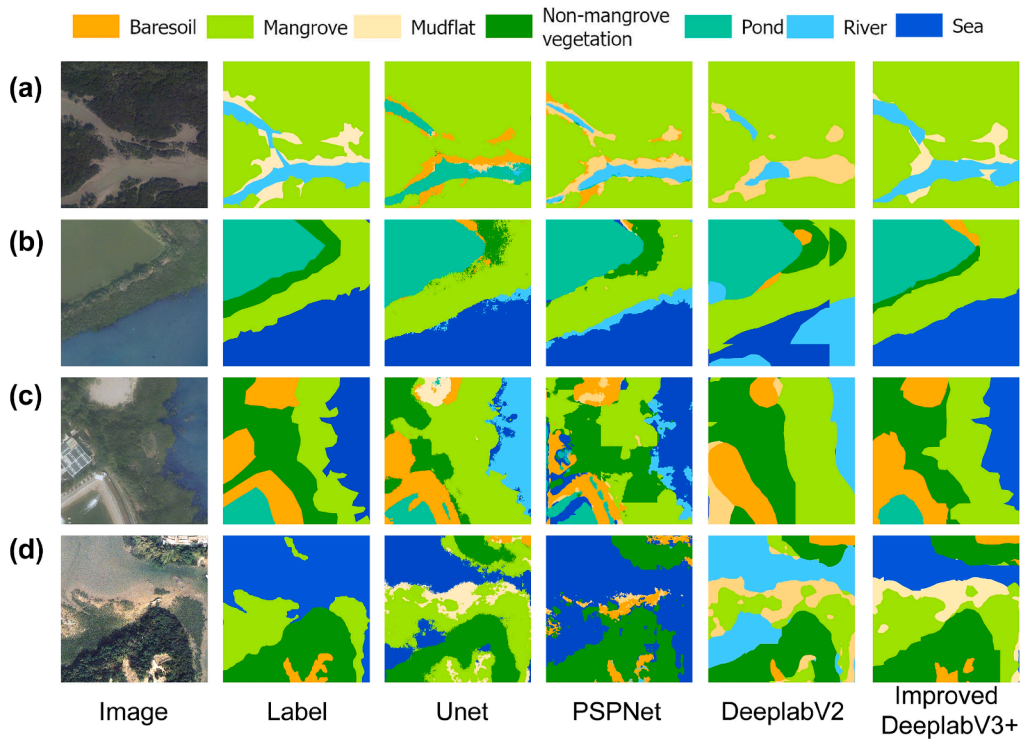

Fig. 11. Spatial comparisons of segmentation results across different models.

estuary, brackish zones near aquaculture ponds, bays, and islands (Fig. 11(a)-(d)). Referring to ground-truth labels, the DeepLabV3+ model consistently outperformed its counterparts, particularly in boundary refinement and detail preservation. For instance, PSPNet showed evident misclassification in regions such as islands (Fig. 11(d)), where mangroves were entirely undetected, leading to omission errors. Similarly, DeeplabV2 struggled with mangroves along Hong Kong's east coast (Fig. 11(b)), resulting in overly smoothed edges or jagged artifacts. In contrast, the DeepLabV3+ model significantly mitigated these issues, delivering better accuracy in complex, fragmented, or linear mangrove habitats.

Nevertheless, mangrove classification still poses inherent challenges due to complex edge structures, fragmented habitats, and intertidal dynamics, which require robust models to ensure accurate boundary delineation. While the DeepLabV3+ model effectively mitigated many of these issues, challenges such as edge misclassification and over-segmentation of similar vegetation types, including reed beds and fragmented mangrove patches, persist. Future improvements could focus on enhancing feature extraction through advanced techniques such as attention mechanisms, incorporating additional data like spectral bands and structural parameters (e.g., tree height), and improving feature fusion between shallow and deep layers. By addressing these aspects, the model could better capture the intricate details of mangrove patches in ecologically complex environments, ensuring more reliable classification and enhanced adaptability to intertidal conditions.

6. Conclusions

This study represents the first effort to apply deep learning methods for mangrove mapping in Hong Kong, achieving remarkable results with the DeepLabV3+ model. The model attained an overall accuracy (OA) of 92.1 %, with user accuracy (UA) and producer accuracy (PA) reaching 94.5 % and 92.7 %, respectively. The improved DeepLabV3+ outperformed UNet and PSPNet, particularly in precision, with improvements of 24 %, 16 %, and 19 %, respectively. Compared to existing datasets, the results showcased significant advancements in spatial detail, including boundary reconstruction, background delineation in complex natural and human-modified settings, and the preservation of internal patch structures.

A novel framework was proposed to quantify scale effects, revealing insights into accuracy and area estimation at various scales. Analysis of patch width indicated 6 m as the optimal scale, with its ecological significance supported by better resolution alignment to fragmented mangrove habitats. Beyond 6 m, accuracy dropped sharply, first within the 10 m range and then accelerating when transitioning to 30 m, where accuracy fell to as low as 0.7 across the study area and 0.66 in fragmented regions. In habitats dominated by fragmented mangroves, each 1 m increase in resolution resulted in an average underestimation of 5000 m^2 in area and up to 38 % loss in accuracy. While resolutions finer than 10 m can reduce accuracy loss overall, some mangrove habitats still experience $>$ 15 % accuracy degradation.

This study underscores the importance of fine-scale mapping in accurately representing mangroves and the necessity of addressing scale-induced uncertainties. The results offer implications for ecosystem conservation, sustainable management, and policy-making.

CRediT authorship contribution statement

Hanwen Zhang: Writing – original draft, Visualization, Methodology, Data curation, Conceptualization. **Shan Wei:** Writing – review & editing, Software. **Xindan Liang:** Writing – review & editing, Software. **Yiping Chen:** Writing – review & editing, Software, Resources. **Hongsheng Zhang:** Writing – review & editing, Supervision, Project administration, Methodology, Funding acquisition, Data curation.

Declaration of competing interest

The authors declare that they have no known competing financial interests or personal relationships that could have appeared to influence the work reported in this paper.

Acknowledgements

This study was jointly supported by the Research Grants Council (RGC) of Hong Kong, China (HKU27602020, HKU17613022); the National Natural Science Foundation of China (42071390), China; the Shenzhen Science and Technology Program (JCYJ20210324124013037), Shenzhen, China; and the Seed Funding for Strategic Interdisciplinary Research Scheme of The University of Hong Kong, Hong Kong, China.

Data availability

Data will be made available on request.

References

Aplin, P., n.d. On scales and dynamics in observing the environment.

Bryan-Brown, D.N., Connolly, R.M., Richards, D.R., Adame, F., Friess, D.A., Brown, C.J., 2020. Global trends in mangrove forest fragmentation. Sci. Rep. 10, 7117. https://doi.org/10.1038/s41598-020-63880-1.

Carbonneau, P.E., Dugdale, S.J., Breckon, T.P., Dietrich, J.T., Fonstad, M.A., Miyamoto, H., Woodget, A.S., 2020. Adopting deep learning methods for airborne RGB fluvial scene classification. Remote Sens. Environ. 251, 112107. https://doi.org/10.1016/j.rse.2020.112107.

Chen, L.-C., Papandreou, G., Schroff, F., Adam, H., 2017. Rethinking Atrous Convolution for Semantic Image Segmentation.

Du, S., Du, S., Liu, B., Zhang, X., 2021. Incorporating DeepLabv3+ and object-based image analysis for semantic segmentation of very high resolution remote sensing images. Int. J. Digit. Earth 14, 357–378. https://doi.org/10.1080/17538947.2020.1831087.

Feller, I.C., Friess, D.A., Krauss, K.W., Lewis, R.R., 2017. The state of the world's mangroves in the 21st century under climate change. Hydrobiologia 803, 1–12. https://doi.org/10.1007/s10750-017-3331-z.

Feng, G., Ming, D., Wang, M., Yang, J., 2017. Connotations of pixel-based scale effect in remote sensing and the modified fractal-based analysis method. Comput. Geosci. 103, 183–190. https://doi.org/10.1016/j.cageo.2017.03.014.

Friess, D.A., Rogers, K., Lovelock, C.E., Krauss, K.W., Hamilton, S.E., Lee, S.Y., Lucas, R., Primavera, J., Rajkaran, A., Shi, S., 2019. The State of the World's Mangrove Forests: Past, Present, and Future. Annu. Rev. Environ. Resour. 44, 89–115. https://doi.org/10.1146/annurev-environ-101718-033302.

Giri, C., Ochieng, E., Tieszen, L.L., Zhu, Z., Singh, A., Loveland, T., Masek, J., Duke, N., 2011. Status and distribution of mangrove forests of the world using earth observation satellite data. Glob. Ecol. Biogeogr. 20, 154–159. https://doi.org/10.1111/j.1466-8238.2010.00584.x.

Goldberg, L., Lagomasino, D., Thomas, N., Fatoyinbo, T., 2020. Global declines in human-driven mangrove loss. Glob. Change Biol. 26, 5844–5855. https://doi.org/10.1111/gcb.15275.

Gonzalez-Perez, A., Abd-Elrahman, A., Wilkinson, B., Johnson, D.J., Carthy, R.R., 2022. Deep and machine learning image classification of coastal wetlands using unpiloted aircraft system multispectral images and lidar datasets. Remote Sens. 14, 3937. https://doi.org/10.3390/rs14163937.

Guo, Y., Liao, J., Shen, G., 2021. Mapping large-scale mangroves along the maritime silk road from 1990 to 2015 using a novel deep learning model and landsat data. Remote Sens. 13, 245. https://doi.org/10.3390/rs13020245.

He, J., Wang, C., Zhang, W., Wang, X., Guo, H., Xue, Q., 2024. An improved DeepLab V3 + for wetland mapping. Sci. Surv. Mappingin Chin. 49, 87–97. https://doi.org/10.16251/j.cnki.1009-2307.2024.03.010.

Hong, Y., Que, X., Wang, Z., Ma, X., Wang, H., Salati, S., Liu, J., 2024. Mangrove extraction from super-resolution images generated by deep learning models. Ecol. Indic. 159, 111714. https://doi.org/10.1016/j.ecolind.2024.111714.

Jia, M., Wang, Z., Mao, D., Ren, C., Song, K., Zhao, C., Wang, C., Xiao, X., Wang, Y., 2023. Mapping global distribution of mangrove forests at 10-m resolution. Sci. Bull. 68, 1306–1316. https://doi.org/10.1016/j.scib.2023.05.004.

Lam, N.-S.-N., Quattrochi, D.A., 1992. On the issues of Scare, Resolution, and Fractal Analysis in the Mapping Sciences. Prof. Geogr. 44, 88–98. https://doi.org/10.1111/j.0033-0124.1992.00088.x.

Lovelock, C.E., Cahoon, D.R., Friess, D.A., Guntenspergen, G.R., Krauss, K.W., Reef, R., Rogers, K., Saunders, M.L., Sidik, F., Swales, A., Saintilan, N., Thuyen, L.X., Triet, T., 2015. The vulnerability of Indo-Pacific mangrove forests to sea-level rise. Nature 526, 559–563. https://doi.org/10.1038/nature15538.

Mahdianpari, M., Granger, J.E., Mohammadimanesh, F., Warren, S., Puestow, T., Salehi, B., Brisco, B., 2021. Smart solutions for smart cities: Urban wetland mapping using very-high resolution satellite imagery and airborne LiDAR data in the City of St. John's, NL, Canada. J. Environ. Manage. 280, 111676. Doi: 10.1016/j.jenvman.2020.111676.

Mallick, J., Talukdar, S., Shahfahad, P.S., Rahman, A., 2021. A novel classifier for improving wetland mapping by integrating image fusion techniques and ensemble machine learning classifiers. Ecol. Inform. 65, 101426. https://doi.org/10.1016/j.ecoinf.2021.101426.

Marceau, D.J., Hay, G.J., 1999. Remote Sensing Contributions to the Scale Issue. Can. J. Remote Sens. 25, 357–366. https://doi.org/10.1080/07038992.1999.10874735.

Onishi, M., Ise, T., 2021. Explainable identification and mapping of trees using UAV RGB image and deep learning. Sci. Rep. 11, 903. https://doi.org/10.1038/s41598-020-79653-9.

Romañach, S.S., DeAngelis, D.L., Koh, H.L., Li, Y., Teh, S.Y., Raja Barizan, R.S., Zhai, L., 2018. Conservation and restoration of mangroves: Global status, perspectives, and prognosis. Ocean Coast. Manag. 154, 72–82. https://doi.org/10.1016/j.ocecoaman.2018.01.009.

Tian, J., Zhang, Y., Diao, C., Le, W., Zhu, L., Xu, M., Song, J., Qu, X., Li, X., Gong, H., 2024. A First National-Scale Sub-Meter Mangrove Map Using a Novel Automatic Sample Collection Method. Doi: Available at SSRN: https://ssrn.com/abstract=4804003 or https://doi.org/10.2139/ssrn.4804003.

Vieilledent, G., Grinand, C., Rakotomalala, F., Ranaivosoa, R., Rakotoarijaona, J., Allnutt, T., Achard, F., 2018. Combining global tree cover loss data with historical national forest cover maps to look at six decades of deforestation and forest fragmentation in Madagascar. Biol. Conserv. 222, 189–197. https://doi.org/10.1016/j.biocon.2018.04.008.

Wang, L., Jia, M., Yin, D., Tian, J., 2019. A review of remote sensing for mangrove forests: 1956-2018. REMOTE Sens. Environ. 231. https://doi.org/10.1016/j.rse.2019.111223.

Wang, Z., Li, J., Tan, Z., Liu, X., Li, M., 2023. Swin-UperNet: A Semantic Segmentation Model for Mangroves and Spartina alterniflora Loisel Based on UperNet. Electronics 12, 1111. https://doi.org/10.3390/electronics12051111.

Wang, X., Xiao, X., Zou, Z., Hou, L., Qin, Y., Dong, J., Doughty, R., Chen, B., Zhang, X., Cheng, Y., Ma, J., Zhao, B., Li, B., 2020. Mapping coastal wetlands of China using time series Landsat images in 2018 and Google Earth Engine. ISPRS J. Photogramm. REMOTE Sens. 163, 312–326. https://doi.org/10.1016/j.isprsjprs.2020.03.014.

Weng, Q., n.d. Scale Issues in Remote Sensing.

Wei, S., Zhang, H., Xu, Z., et al., 2024. Coastal urbanization may indirectly positively impact growth of mangrove forests. Commun Earth Environ 5, 608. https://doi.org/10.1038/s43247-024-01776-y.

Woodcock, C.E., Strahler, A.H., 1987. The factor of scale in remote sensing. Remote Sens. Environ. 21, 311–332. https://doi.org/10.1016/0034-4257(87)90015-0.

Yao, X., Yang, H., Wu, Y., Wu, P., Wang, B., Zhou, X., Wang, S., 2019. Land use classification of the deep convolutional neural network method reducing the loss of spatial features. Sensors 19, 2792. https://doi.org/10.3390/s19122792.

Yu, L., Zeng, Z., Liu, A., Xie, X., Wang, H., Xu, F., Hong, W., 2022. A Lightweight complex-valued DeepLabv3+ for semantic segmentation of PolSAR image. IEEE J. Sel. Top. Appl. Earth Obs. Remote Sens. 15, 930–943. https://doi.org/10.1109/JSTARS.2021.3140101.

Zhang, T., Hu, S., He, Y., You, S., Yang, X., Gan, Y., Liu, A., 2021. A fine-scale mangrove map of china derived from 2-meter resolution satellite observations and field data. ISPRS Int. J. Geo-Inf. 10, 92. https://doi.org/10.3390/ijgi10020092.

Zhao, C., Qin, C.-Z., 2020. 10-m-resolution mangrove maps of China derived from multi-source and multi-temporal satellite observations. ISPRS J. Photogramm. Remote Sens. 169, 389–405. https://doi.org/10.1016/j.isprsjprs.2020.10.001.

Zhao, T., Wang, S., Ouyang, C., Chen, M., Liu, C., Zhang, J., Yu, L., Wang, F., Xie, Y., Li, J., 2024. Artificial intelligence for geoscience: Progress, challenges and perspectives. The Innovation 5 (5), 100691. https://doi.org/10.1016/j.xinn.2024.100691.